Supplementary material

Triple oxygen isotope systematics of evaporation and mixing processes in a dynamic desert lake system

Claudia Voigt[1], Daniel Herwartz[1], Cristina Dorador[2], Michael Staubwasser[1]

[1]Institute of Geology and Mineralogy, University of Cologne, Zülpicher Str. 49b, 50674 Cologne, Germany
[2]Centro de Biotecnología, Universidad de Antofagasta, Angamos 601, 1270300 Antofagasta, Chile

Correspondence to: Claudia Voigt (c.voigt@uni-koeln.de)

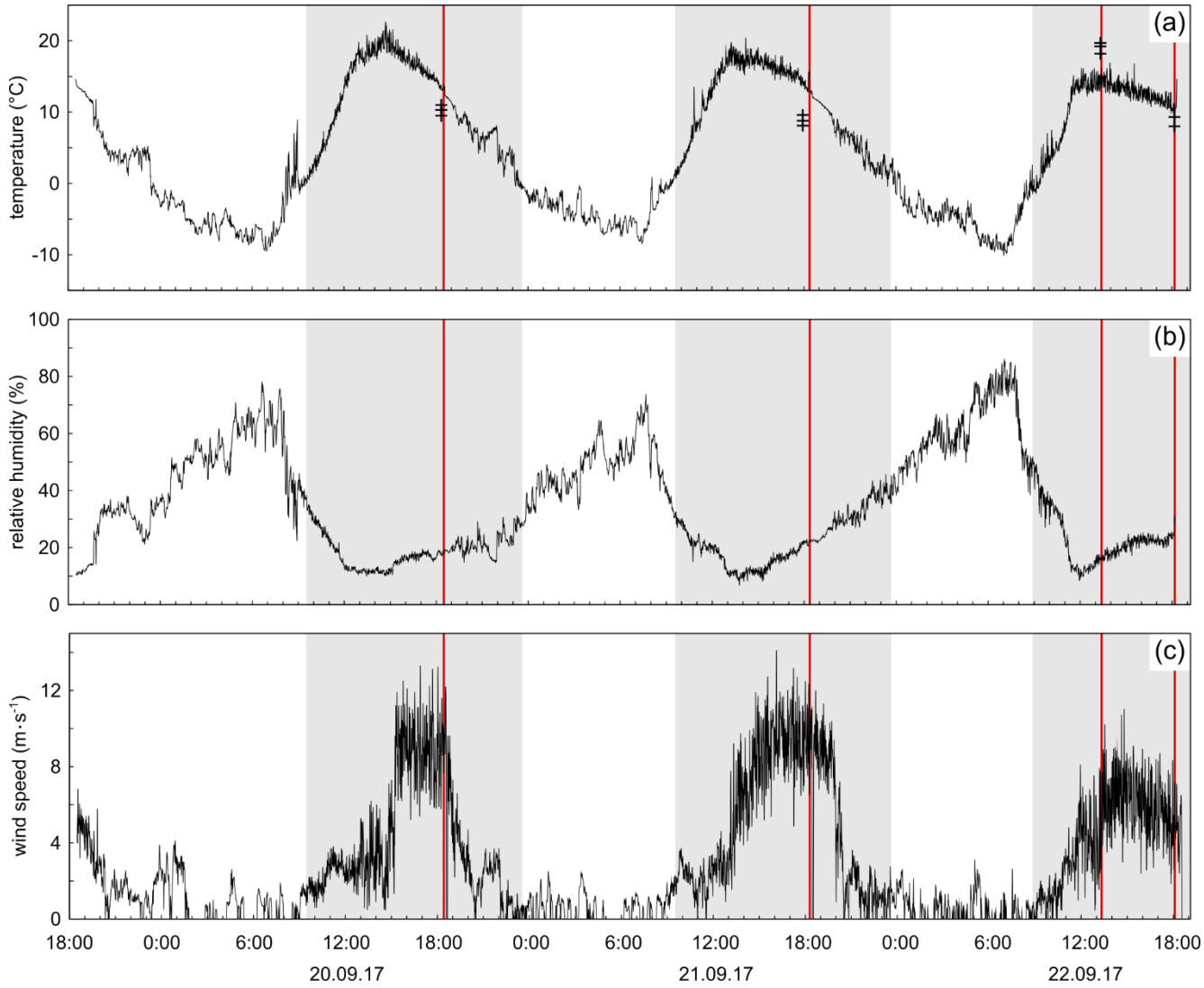

Figure S1: Temperature (a), relative humidity (b), and wind speed (c) measured on site over the period of the evaporation experiment. Shaded areas indicate time intervals, where temperatures exceed 0°C and waters are assumed to be not frozen. Red lines show time of sampling. Crosses in panel A represent water temperatures measured during sampling. While water temperatures are lower than air in the evening, they can exceed air temperatures during midday.

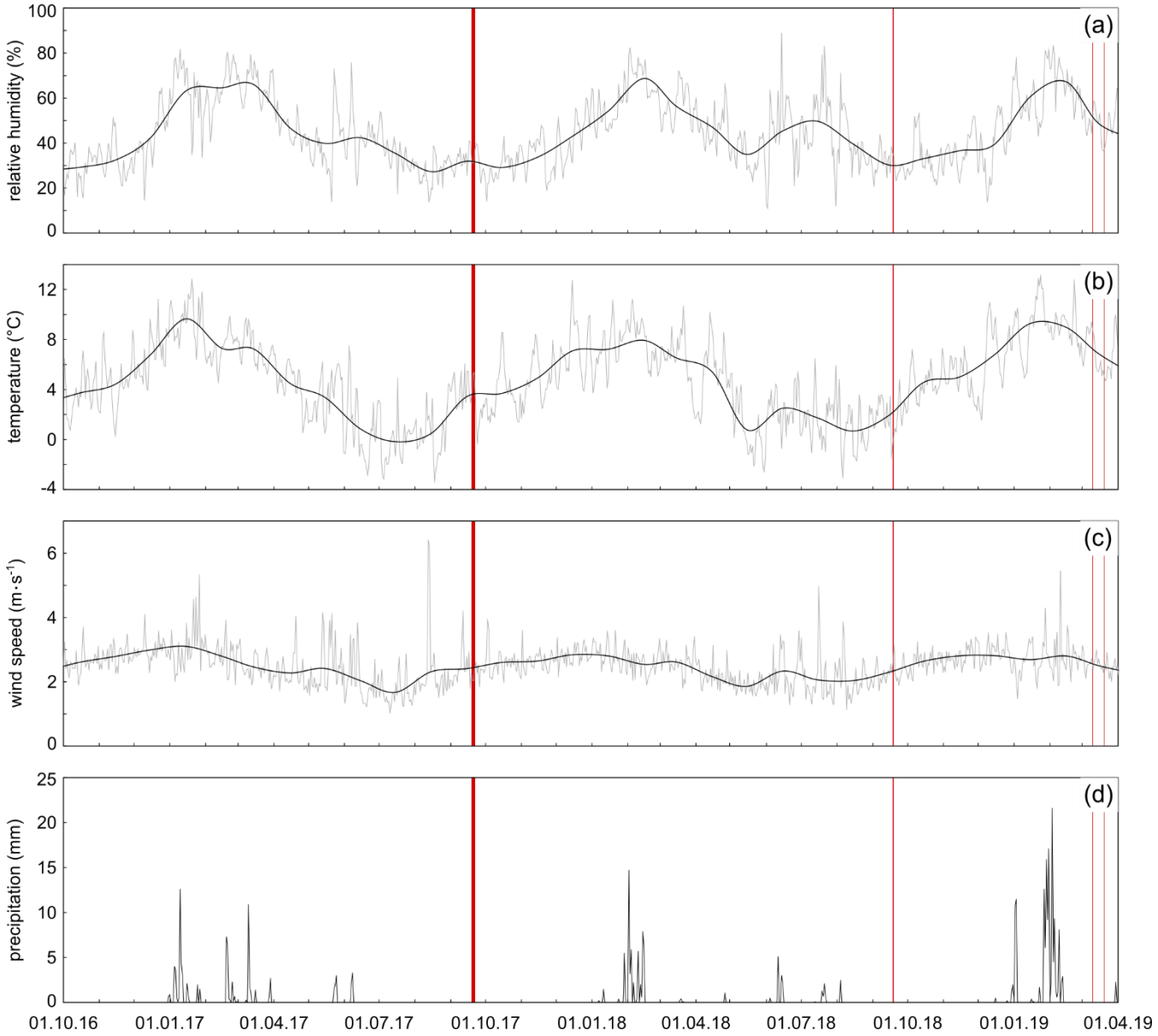

Figure S2: Temperature (a), relative humidity (b), wind speed (b) and precipitation data (d) from the Salar del Huasco weather station (20.257°S 68.873°W, 3804 m a.s.l.) for the period from October 2016 to March 2019 (data from CEAZA, 2019). Black lines in panel (a)-(c) show monthly average conditions, while grey lines illustrate daily variations. Red bars represent days of sampling.

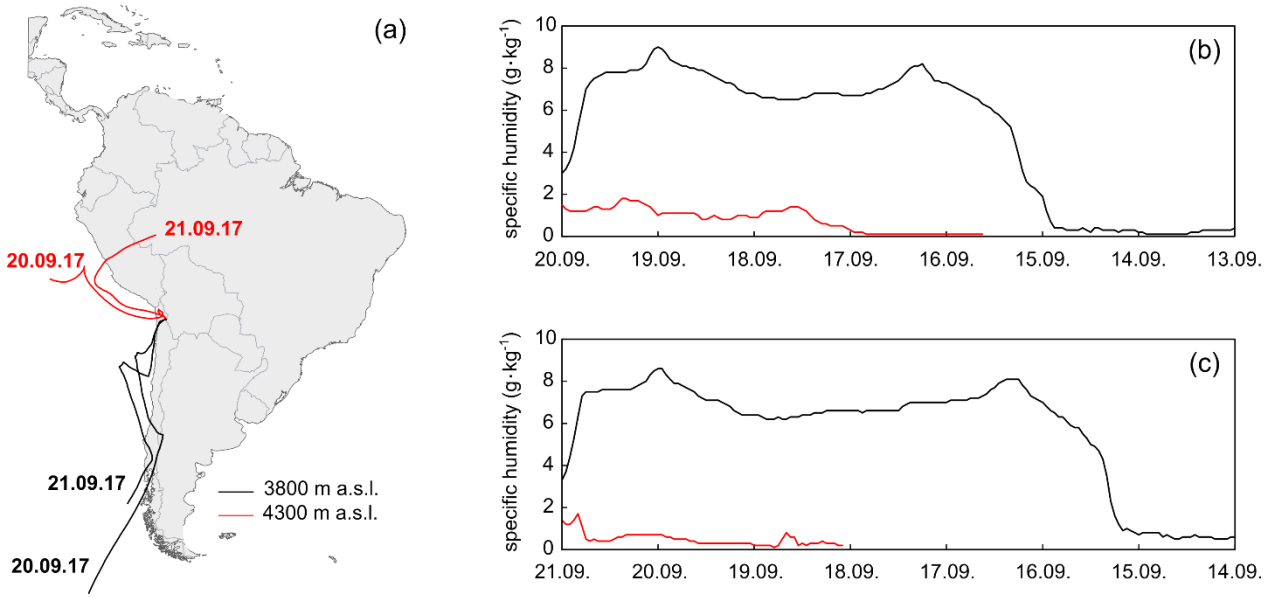

Figure S3: HYSPLIT 7-day air mass back trajectories (A) modelled for ground level (~3800 m above sea level (a.s.l.)) (black) and 1500 m above ground level (5300 m a.s.l.) (red) at the Salar del Huasco for the start time of vapor extractions (18:00) on 20.09.17 and 21.09.2017. Panel (b) and (c) show the specific humidity of the respective air masses.

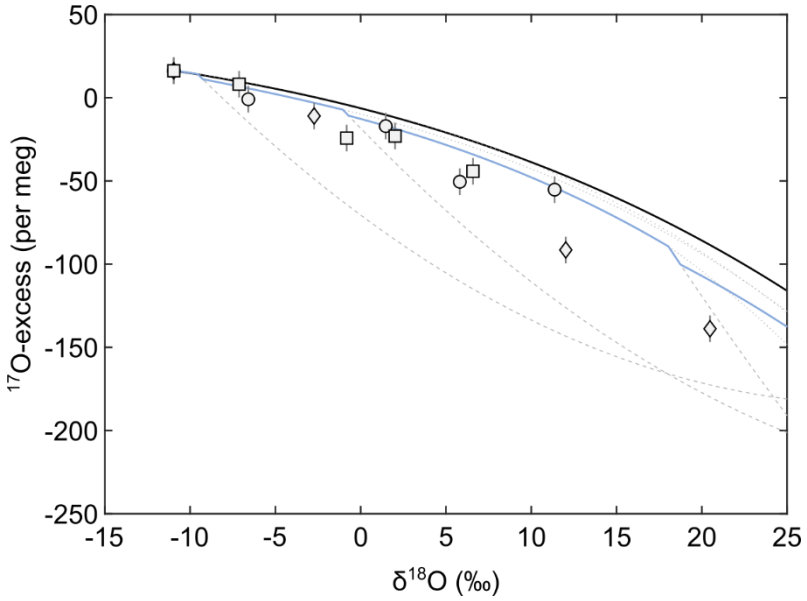

Figure S4: Illustration of isotope effects associated with mixing that might affect the isotopic composition of pan evaporation experiments during thawing. The black curve indicates the simple evaporation trajectory without mixing. The blue curve shows the evaporation trajectory for the example of an initial volume of 600 ml considering mixing during thawing. The curve is modelled using evaporation rates based on measured residual fractions and assuming that 30 ml of the ice thawed in the morning, evaporated to 90 % and mixed with the residual water. Mixing ratios are < 1% at the beginning of the experiment but become significant with decreasing volume of the residual water leading to an overall lowering of ^{17}O-excess of evaporated pan waters with respect to the predicted simple evaporation trajectory.

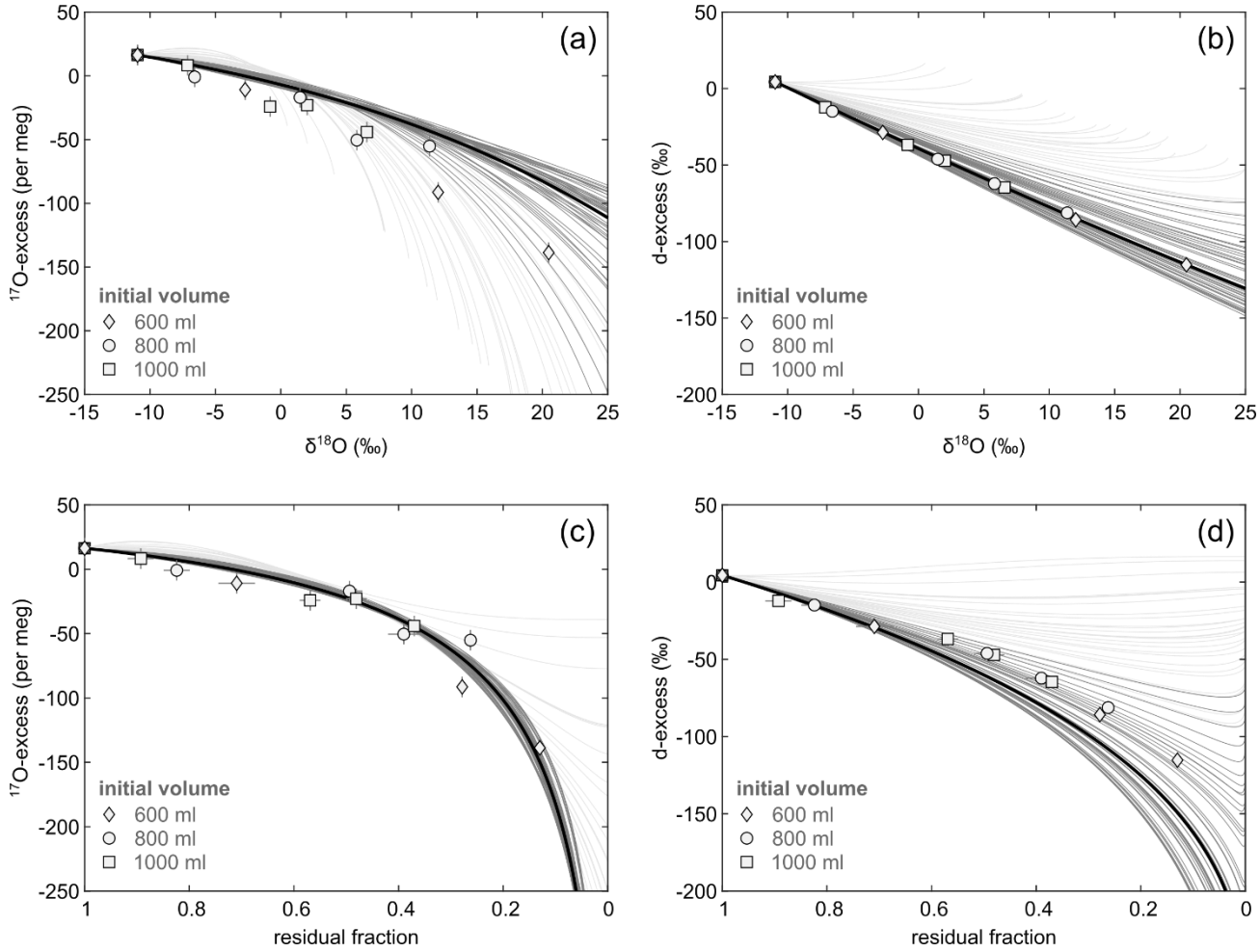

Figure S5: Diagrams of ^{17}O-excess and d-excess over ((a) and (b)) δ^{18}O and ((c) and (d)) residual fraction for pan evaporation experiments with initial volume of 600 ml (diamonds), 800 ml (circles), 1000 ml (squares). Note that the symbol size can be larger than the error bars. Simple evaporation trajectories were modelled in hourly resolution for the period of the evaporation experiment (dark grey lines for hourly average T > 0°C and light grey lines for hourly average T < 0°C). The solid black line represents the mean simple evaporation trajectory for T > 0°C. The model input parameters are summarized in Table 1 in the main text.

T1 Hydrogeochemical composition

Natural waters in the Salar del Huasco span a wide range in total dissolved solids (TDS) from 0.4 $g \cdot l^{-1}$ up to 343 $g \cdot l^{-1}$. Springs are fresh with an average TDS of 0.7 ± 0.5 $g \cdot l^{-1}$. Ponds in the SE and NW areas of the Salar del Huasco comprise generally low salinity in the range of brackish waters. Hypersaline waters are observed in the N area with most of the ponds having TDS values higher than 100 $g \cdot l^{-1}$.

Major ion analyses reveal that the waters originate from two source types (Fig. S6). All spring waters are dominated by calcium and sodium. However, springs at the western margin of the salar are of bicarbonate composition, while the spring at the south-eastern end of the salar classify as sulfate type. The difference in hydrogeochemical composition of spring waters is probably attributed to the aquifers. The calcium-sodium bicarbonate composition of western springs is associated with ignimbrite deposits in the north of the Salar del Huasco (Flores Grandez, 2010). The sulfate-rich composition of the south-eastern spring is linked to volcanic units in the east of the Salar del Huasco (Flores Grandez, 2010).

The hydrogeochemical composition of lakes and ponds is related to their source (Fig. S6). Evaporation leads to the enrichment of the dissolved ions in the waters, precipitation of carbonates, sodium sulfates and chlorides at the saturation limit, and the transition to sodium-chloride type waters. Furthermore, dissolution of older evaporitic units may contribute to the high sodium chloride concentrations especially in the northern area of the Salar del Huasco.

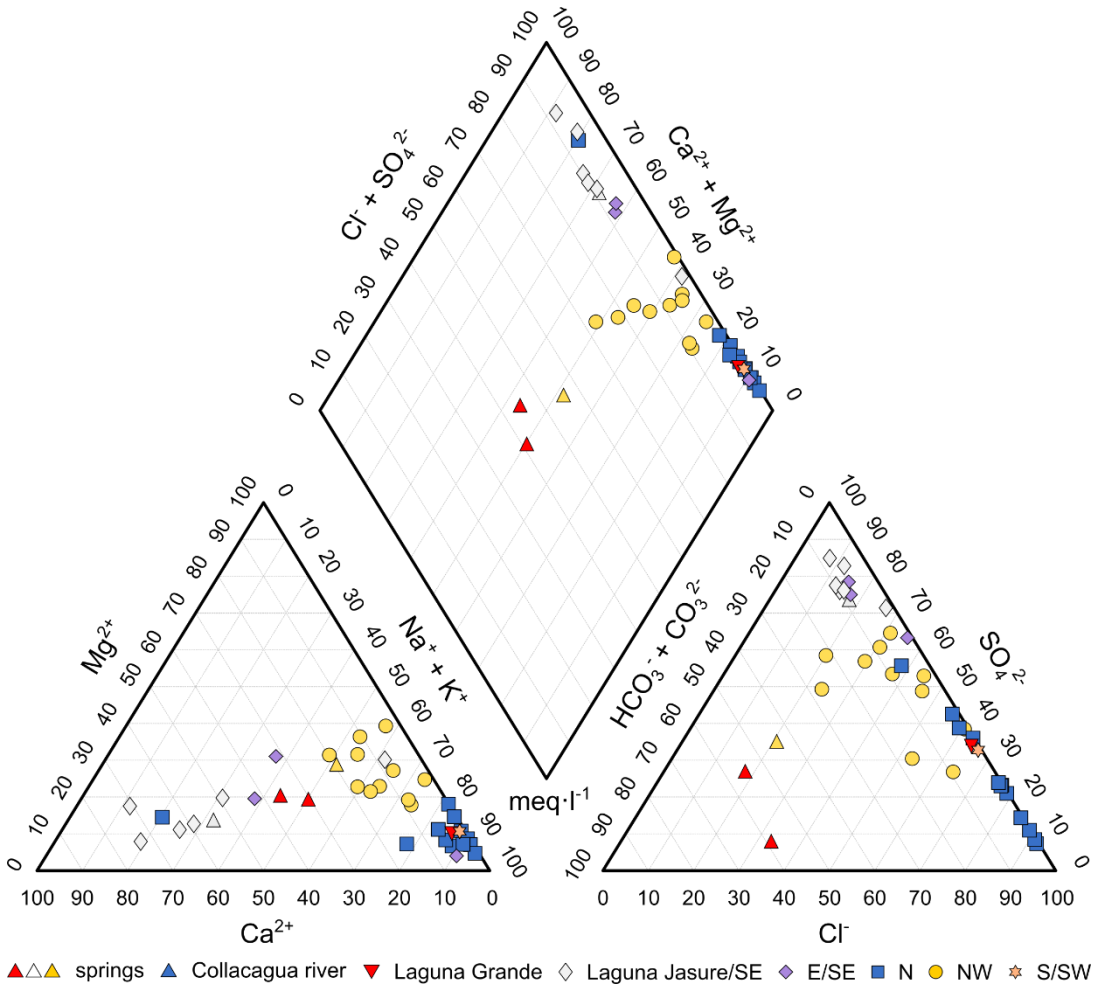

Figure S6: Hydrogeochemical composition of springs, ponds and lakes sampled in 09/17 at the Salar del Huasco. Symbology refers to the corresponding hydrological subsystem.

65

70

Table S1: Hydrogeochemical composition of sampled natural waters.

sample	latitude	longitude	elevation (m asl)	pH	TDS ($g \cdot l^{-1}$)	Na ($g \cdot l^{-1}$)	K ($g \cdot l^{-1}$)	Ca ($g \cdot l^{-1}$)	Mg ($g \cdot l^{-1}$)	Cl ($g \cdot l^{-1}$)	S ($g \cdot l^{-1}$)	HCO_3 ($g \cdot l^{-1}$)	CO_3 ($g \cdot l^{-1}$)
springs													
09/2017													
Ata17-192	20° 15.166' S	68° 52.116' W	3794	7.69	0.44	0.08	0.01	0.02	0.01	0.04	0.04	0.23	0.00
Ata17-212	20° 15.770' S	68° 52.527' W	3776	7.84	0.43	0.06	0.01	0.04	0.01	0.03	0.03	0.25	0.00
Ata17-214	20° 16.983' S	68° 53.366' W	3780	8.04	1.39	0.08	0.01	0.04	0.01	0.20	0.03	1.02	0.01
Ata17-216	20° 20.229' S	68° 48.937' W	3789	7.88	0.38	0.06	0.01	0.09	0.01	0.04	0.11	0.06	0.00
09/2018													
Ata18-044	20° 16.969' S	68° 53.374' W	3779	7.40	0.39	0.07	0.01	0.04	0.01	0.03	0.03	0.21	0.00
Ata18-048	20° 18.307' S	68° 53.273' W	3781	8.20	0.70	0.12	0.01	0.08	0.01	0.08	0.05	0.34	0.01
Ata18-050	20° 18.296' S	68° 53.234' W	3782	8.45	2.11	0.47	0.08	0.09	0.09	0.31	0.24	0.81	0.02
Ata18-063	20° 20.229' S	68° 48.937' W	3789	7.93	0.38	0.07	0.01	0.09	0.01	0.03	0.11	0.05	0.00
Ata18-066	20° 15.165' S	68° 52.114' W	3793	7.72	0.42	0.08	0.01	0.05	0.01	0.03	0.05	0.19	0.00
Ata18-069	20° 16.565' S	68° 53.210' W	3787	8.76	0.34	0.07	0.00	0.03	0.01	0.04	0.02	0.17	0.00
Ata18-070	20° 15.770' S	68° 52.527' W	3776	7.80	0.40	0.07	0.01	0.04	0.01	0.03	0.03	0.20	0.00
03/2019													
Ata19-024	20° 20.228' S	68° 48.939' W	3788	8.26	-	-	-	-	-	-	-	-	-
Ata19-035	20° 20.220' S	68° 50.299' W	3785	-	-	-	-	-	-	-	-	-	-
Ata19-116	20° 15.165' S	68° 52.115' W	3793	7.83	0.55	0.11	0.02	0.05	0.01	0.08	0.06	0.20	0.00
Ata19-123	20° 15.745' S	68° 52.556' W	3793	8.12	-	-	-	-	-	-	-	-	-
Ata19-126	20° 16.986' S	68° 53.358' W	3782	8.02	0.38	0.07	0.01	0.04	0.01	0.04	0.03	0.19	0.00
Collacagua river													
09/2018													
Ata18-065	20° 06.175' S	68° 50.603' W	3855	8.35	0.48	0.07	0.01	0.04	0.02	0.03	0.02	0.28	0.01
03/2019													
Ata19-021	20° 06.171' S	68° 50.603' W	3850	8.28	0.51	0.07	0.01	0.05	0.02	0.03	0.03	0.29	0.00
Laguna Grande													
09/2017													
Ata17-213	20° 16.422' S	68° 52.974' W	3777	8.74	19.75	6.92	1.24	0.21	0.24	7.95	2.59	0.59	0.01
09/2018													
Ata18-089	20° 16.433' S	68° 53.034' W	3785	8.42	-	-	-	-	-	-	-	-	-
03/2019													
Ata19-124	20° 16.427' S	68° 53.047' W	3784	8.73	36.23	13.24	2.28	0.60	0.33	13.24	5.90	0.64	0.01
NW area													
03/2017													
Ata17-181a	20° 15.510' S	68° 52.122' W	2788	8.87	0.63	0.14	0.02	0.05	0.03	0.07	0.09	0.23	0.00
Ata17-182	20° 15.533' S	68° 51.971' W	3787	8.67	6.34	2.15	0.23	0.34	0.22	1.27	1.62	0.50	0.00
Ata17-183	20° 15.472' S	68° 51.905' W	3786	8.92	2.74	0.94	0.15	0.09	0.07	0.57	0.51	0.41	0.00
Ata17-184	20° 15.454' S	68° 51.963' W	3788	8.44	3.20	0.92	0.07	0.21	0.10	0.53	0.64	0.72	0.00
Ata17-185	20° 15.516' S	68° 51.966' W	3789	8.71	3.40	1.06	0.10	0.21	0.10	0.64	0.78	0.51	0.00
Ata17-186	20° 15.398' S	68° 51.968' W	3789	8.36	3.52	1.09	0.05	0.10	0.08	1.30	0.34	0.56	0.00
Ata17-187	20° 15.301' S	68° 52.007' W	3790	8.81	1.12	0.30	0.04	0.05	0.06	0.11	0.21	0.35	0.00
Ata17-188	20° 15.191' S	68° 51.996' W	3792	8.49	39.78	11.83	2.53	0.55	2.40	15.64	6.15	0.68	0.00
Ata17-189a	20° 15.188' S	68° 51.972' W	3791	8.58	8.32	2.65	0.27	0.24	0.32	2.45	1.61	0.78	0.00
Ata17-190	20° 15.159' S	68° 52.010' W	3794	8.64	24.66	8.97	1.35	0.20	0.88	6.95	5.12	1.18	0.01
Ata17-191	20° 15.180' S	68° 52.102' W	3793	8.48	1.11	0.22	0.05	0.04	0.04	0.34	0.12	0.30	0.00

(continued)

sample	latitude	longitude	elevation (m asl)	pH	TDS ($g \cdot l^{-1}$)	Na ($g \cdot l^{-1}$)	K ($g \cdot l^{-1}$)	Ca ($g \cdot l^{-1}$)	Mg ($g \cdot l^{-1}$)	Cl ($g \cdot l^{-1}$)	S ($g \cdot l^{-1}$)	HCO_3 ($g \cdot l^{-1}$)	CO_3 ($g \cdot l^{-1}$)
N area													
03/2017													
Ata17-194	20° 17.814' S	68° 49.605' W	3796	7.39	343.11	95.64	38.40	0.07	6.65	189.87	9.34	3.14	0.00
Ata17-195	20° 17.795' S	68° 49.600' W	3797	7.67	268.56	79.00	24.45	0.38	4.18	149.99	8.63	1.93	0.00
Ata17-196	20° 17.815' S	68° 49.644' W	3798	7.73	236.00	71.55	18.96	0.61	2.64	131.02	10.04	1.18	0.00
Ata17-197a	20° 17.816' S	68° 49.639' W	3796	7.85	245.76	82.71	18.30	0.38	2.35	120.83	19.92	1.26	0.00
Ata17-198	20° 17.765' S	68° 49.681' W	3792	7.94	201.42	69.47	16.53	0.43	1.60	94.58	17.84	0.96	0.00
Ata17-199	20° 17.765' S	68° 49.686' W	3794	7.93	181.61	69.67	9.92	0.53	1.00	73.90	25.86	0.73	0.00
Ata17-200a	20° 17.740' S	68° 49.700' W	3791	9.29	65.01	20.00	5.00	0.92	0.46	31.99	5.97	0.67	0.00
Ata17-201	20° 17.726' S	68° 49.731' W	3789	9.10	51.30	15.80	4.44	0.85	0.46	24.36	4.79	0.60	0.00
Ata17-202	20° 17.715' S	68° 49.743' W	3790	8.95	11.75	3.68	1.13	0.58	0.10	4.02	1.90	0.33	0.00
Ata17-203	20° 17.716' S	68° 59.759' W	3790	9.12	113.75	36.61	7.89	0.74	0.86	60.35	6.31	0.97	0.01
Ata17-204	20° 17.663' S	68° 49.818' W	3786	8.87	31.30	10.14	3.46	0.60	0.42	11.13	4.51	1.02	0.01
Ata17-205	20° 17.578' S	68° 49.838' W	3789	8.56	2.12	0.19	0.05	0.51	0.04	0.56	0.50	0.27	0.00
03/2019													
Ata19-115	20° 17.578' S	68° 50.071' W	3784	8.27	149.68	45.00	18.75	0.72	1.05	69.47	14.67	0.01	0.02
SE area													
09/2017													
Ata17-217	20° 20.045' S	68° 49.034' W	3789	8.55	0.82	0.11	0.03	0.23	0.01	0.07	0.23	0.14	0.00
Ata17-219	20° 19.730' S	68° 49.081' W	3791	9.20	0.59	0.09	0.02	0.15	0.01	0.05	0.17	0.10	0.00
Ata17-220	20° 19.408' S	68° 49.437' W	3793	8.84	1.10	0.13	0.02	0.39	0.02	0.08	0.36	0.11	0.00
Ata17-222	20° 19.110' S	68° 49.006' W	3793	9.53	17.65	7.24	1.27	0.34	0.09	3.98	4.38	0.34	0.00
Ata17-223	20° 19.114' S	68° 48.990' W	3793	9.63	0.81	0.15	0.06	0.14	0.02	0.09	0.23	0.12	0.00
Ata17-224	20° 19.122' S	68° 49.006' W	3792	7.89	3.80	0.78	0.29	0.56	0.20	0.36	1.15	0.46	0.00
Ata17-225	20° 19.615' S	68° 48.978' W	3789	8.71	0.69	0.12	0.02	0.15	0.02	0.06	0.20	0.11	0.00
Ata17-226	20° 19.749' S	68° 48.962' W	3791	8.37	1.62	0.11	0.03	0.58	0.05	0.08	0.54	0.22	0.00
Ata17-227	20° 19.856' S	68° 48.966' W	3790	8.48	14.76	4.77	1.26	0.51	0.70	2.64	4.35	0.51	0.00
03/2019													
Ata19-031	20° 19.212' S	68° 49.099' W	3781	8.88	95.98	31.62	11.32	0.63	0.91	35.36	15.27	0.84	0.02
Ata19-032	20° 19.353' S	68° 49.059' W	3782	9.40	77.90	26.05	8.58	0.63	1.26	26.52	13.67	1.13	0.05
Ata19-033	20° 19.531' S	68° 49.034' W	3783	9.15	67.34	23.95	4.56	0.86	3.48	14.19	17.86	2.35	0.08
SW area													
09/2017													
Ata17-215	20° 19.335' S	68° 51.803' W	3778	8.39	117.75	40.67	8.32	0.58	1.44	49.53	15.05	2.13	0.02
09/2018													
Ata18-046a	20° 18.322' S	68° 53.300' W	3782	9.50	1.49	0.36	0.04	0.04	0.05	0.22	0.12	0.64	0.01
Ata18-052	20° 18.298' S	68° 53.093' W	3783	8.56	58.43	18.71	4.33	0.58	0.83	27.40	5.78	0.78	0.01
Ata18-053a	20° 18.227' S	68° 53.284' W	3786	9.59	1.50	0.40	0.07	0.02	0.03	0.21	0.12	0.63	0.02
Ata18-056	20° 19.323' S	68° 51.831' W	3786	142.73	52.58	9.32	0.53	1.68	54.54	21.70	2.35	0.02	142.73
Ata18-058	20° 19.418' S	68° 51.726' W	3787	8.42	102.64	37.72	6.78	0.59	1.30	40.83	14.97	0.44	0.01
Ata18-061	20° 19.426' S	68° 51.775' W	3790	8.01	9.94	3.71	0.63	0.37	0.23	2.08	2.51	0.39	0.01
03/2019													
Ata19-038	20° 18.286' S	68° 53.240' W	3788	-	-	-	-	-	-	-	-	-	-

Table S2: Hydrogen and oxygen isotope data derived from pan evaporation experiments.

sample	$\delta^{17}O$ (‰)	SD	$\delta^{18}O$ (‰)	SD	^{17}O-excess (per meg)	SD	n	$\delta^{2}H$ (‰)	SD	d-excess (‰)	n
initial water	-5.79	0.24	-10.96	0.39	16	6	9	-83.3	1.4	4.4	4
600 ml											
1a	-1.45	0.26	-2.73	0.54	-11	30	7	-50.5	0.5	-27.7	3
1b	6.24	0.29	12.03	0.58	-91	35	7	10.4	0.5	-85.8	3
1c	10.62	0.18	20.48	0.30	-139	36	7	48.6	0.5	-115.2	3
800 ml											
2a	-3.48	0.02	-6.59	0.04	-1	4	3	-67.4		-14.7	1
2b	0.75	0.02	1.47	0.02	-17	6	4	-34.5		-46.2	1
2c	3.01	0.17	5.81	0.32	-50	2	3	-15.7		-62.2	1
2d	5.93	0.22	11.37	0.39	-55	18	3	9.8		-81.2	1
1000 ml											
3a	-3.76	0.05	-7.13	0.10	8	0	3	-69.8		-12.8	1
3b	-0.46	0.02	-0.82	0.06	-24	11	3	-43.7		-37.1	1
3c	1.04	0.01	2.02	0.02	-23	5	2	-31.0		-47.1	1
3d	3.43	0.09	6.58	0.13	-44	17	3	-11.9		-64.6	1

Table S3: Hydrogen and oxygen isotope data of sampled lakes and ponds.

sample	$\delta^{17}O$ (‰)	SD	$\delta^{18}O$ (‰)	SD	^{17}O-excess (per meg)	SD	n	$\delta^{2}H$ (‰)	SD	d-excess (‰)	SD	n
springs												
09/2017												
Ata17-192	-6.22	0.02	-11.75	0.04	3	5	2	-95.0	0.8	-1.0		2
Ata17-212	-6.51	0.00	-12.31	0.02	10	6	2	-96.7	1.4	1.8		2
Ata17-214	-6.58	0.18	-12.46	0.36	17	17	5	-97.8	0.4	1.9		2
Ata17-216	-7.02	0.05	-13.28	0.09	15	3	2	-100.2	0.7	6.0		2
mean	**-6.58**	**0.33**	**-12.45**	**0.64**	**11**	**7**		**-97.4**	**2.2**	**2.2**	**2.9**	
09/2018												
Ata18-044	-6.58	0.09	-12.43	0.18	3	6	3	-97.7	0.2	1.8		2
Ata18-048	-6.31	0.15	-11.94	0.29	15	5	3	-96.2		-0.7		1
Ata18-050	-6.83	0.14	-12.91	0.23	9	13	3	-101.0		2.3		1
Ata18-063	-6.89	0.10	-13.03	0.16	7	14	3	-99.1	1.2	5.1		2
Ata18-066	-6.17	0.06	-11.66	0.10	6	10	3	-94.8		-1.5		1
Ata18-069	-6.35	0.08	-12.00	0.13	3	13	3	-95.6		0.4		1
Ata18-070	-6.51	0.05	-12.28	0.11	-5	5	3	-96.1	1.9	2.1		2
mean	**-6.52**	**0.27**	**-12.32**	**0.51**	**5**	**6**		**-97.2**	**2.2**	**1.4**	**2.2**	
03/2019												
Ata19-024	-6.99	0.02	-13.22	0.04	9	3	2	-99.4		6.3		1
Ata19-035	-6.96	0.01	-13.16	0.01	6	5	2	-99.1		6.1		1
Ata19-116	-6.14	0.11	-11.59	0.22	-1	4	3	-87.3		5.4		1
Ata19-123	-6.57	0.02	-12.41	0.04	3	0	2	-97.1		2.2		1
Ata19-126	-6.57	0.07	-12.39	0.15	-6	5	3	-91.7		7.4		1
mean	**-6.65**	**0.35**	**-12.55**	**0.68**	**2**	**6**		**-94.9**	**5.3**	**5.5**	**2.0**	
Collacagua river												
09/2018												
Ata18-065	-6.55	0.03	-12.38	0.07	5	9	4	-97.5		1.6		1
03/2019												
Ata19-021	-6.59	0.04	-12.45	0.05	5	15	4	-93.8		5.8		1
Laguna Grande												
09/2017												
Ata17-213	-1.35	0.01	-2.48	0.03	-37	2	2	-49.2	0.0	-29.4		2
09/2018												
Ata18-089	1.65	0.08	3.20	0.13	-39	7	3	-16.3	0.5	-41.9		1
03/2019												
Ata19-124	-2.20	0.10	-4.14	0.18	-15	4	3	-55.1		-21.9		1
NW area												
09/2017												
Ata17-181a	-5.24	0.01	-9.90	0.02	3	4	2	-87.5	0.8	-8.2		2
Ata17-182	-4.07	0.07	-7.69	0.11	-4	13	3	-76.0	0.6	-14.5		2
Ata17-183	-4.00	0.01	-7.55	0.02	-3	2	2	-75.8	0.5	-15.4		2
Ata17-184	-4.89	0.01	-9.26	0.01	12	6	2	-84.6	1.3	-10.5		2
Ata17-185	-4.76		-9.00		7		1	-82.8	1.5	-10.8		2
Ata17-186	-4.54	0.02	-8.59	0.04	2	0	2	-81.3	0.2	-12.6		2
Ata17-187	-4.37		-8.27		11		1	-77.6	0.1	-11.5		2
Ata17-188	-1.06	0.06	-1.94	0.12	-32	9	2	-51.5		-35.9		1
Ata17-189a	-1.85	0.06	-3.46	0.10	-21	7	3	-57.7	0.1	-30.0		2

Ata17-190	-1.26	0.01	-2.31	0.01	-39	1	2	-53.6		-35.0	1
Ata17-191	-3.67	0.06	-6.91	0.10	-11	7	2	-70.7	1.0	-15.4	2
N area											
09/2017											
Ata17-194	0.04	0.02	0.17	0.04	-54	2	2	-37.4	5.3	-38.8	2
Ata17-195	-0.52	0.18	-0.90	0.35	-38	8	2	-50.2	2.7	-42.9	2
Ata17-196	-0.64	0.08	-1.11	0.16	-50	4	2	-52.5	3.3	-43.6	2
Ata17-197a	-1.20	0.06	-2.21	0.12	-34	6	3	-54.7		-37.1	1
Ata17-198	-1.27	0.00	-2.33	0.01	-36	2	2	-57.5		-38.8	1
Ata17-199	-2.53	0.01	-4.74	0.01	-25	3	2	-65.2		-27.3	1
Ata17-200a	1.96	0.05	3.85	0.09	-67	7	3	-27.5	1.3	-58.3	2
Ata17-201	1.48	0.00	2.94	0.00	-73	4	2	-30.0	1.4	-53.5	2
Ata17-202	-5.63	0.09	-10.65	0.17	7	1	2	-90.4	0.9	-5.3	1
Ata17-203	2.24	0.05	4.34	0.12	-54	12	2	-29.7	1.3	-64.4	2
Ata17-204	-0.66	0.02	-1.20	0.04	-29	1	2	-44.4		-34.8	1
Ata17-205	-5.55	0.02	-10.51	0.05	16	4	3	-87.2	1.3	-3.1	2
03/2019											
Ata19-115	0.36	0.14	0.74	0.26	-32	3	2	-36.5		-42.4	1
SE area											
09/2017											
Ata17-217	-4.75	0.13	-9.02	0.25	19	16	4	-81.4	0.7	-9.3	2
Ata17-219	-3.63	0.15	-6.85	0.28	-13	1	2	-73.0	0.1	-18.2	2
Ata17-220	-4.21	0.03	-7.99	0.07	17	8	2	-75.0	0.2	-11.0	2
Ata17-222	-0.95	0.00	-1.75	0.01	-31	8	2	-45.9	0.1	-31.9	2
Ata17-223	-3.95	0.05	-7.47	0.08	5	3	2	-75.4	0.5	-15.7	2
Ata17-224	-4.32	0.00	-8.13	0.01	-21	12	2	-79.5	0.4	-14.5	2
Ata17-225	-5.93	0.03	-11.23	0.04	16	5	2	-91.1	0.1	-1.3	2
Ata17-226	-5.41	0.07	-10.24	0.15	14	9	2	-84.4	0.8	-2.5	2
Ata17-227	-2.21	0.01	-4.15	0.03	-19	5	2	-60.5	0.0	-27.3	2
03/2019											
Ata19-031	-0.47	0.05	-0.87	0.10	-17	3	2	-45.1		-38.1	1
Ata19-032	3.53	0.14	6.76	0.29	-38	13	3	-10.0		-64.1	1
Ata19-033	7.20	0.10	13.89	0.17	-108	5	2	10.7		-100.4	1
SW area											
09/2017											
Ata17-215	6.44	0.11	12.43	0.22	-102	11	4	30.8	0.4	-68.6	2
09/2018											
Ata18-046a	-2.94	0.08	-5.54	0.16	-13	3	4	-69.0		-24.6	1
Ata18-052	4.48	0.04	8.63	0.06	-61	5	2	12.7		-56.3	1
Ata18-053a	-2.70	0.09	-5.09	0.16	-14	4	3	-66.8		-26.1	1
Ata18-056a	7.53	0.05	14.50	0.09	-98	5	4	38.0		-78.0	1
Ata18-058	5.74		10.55		-82		1	18.9	1.3	-65.5	2
Ata18-061	-2.33	0.03	-4.40	0.05	-11	1	3	-57.9		-22.8	1
03/2019											
Ata19-038	-0.32	0.01	-0.56	0.02	-24	0	2	-43.2		-38.7	1

References

CEAZA, (Centro de Estudios Avanzados en Zonas Áridas), 2019. Estación Salar de Huasco. http://www.ceazamet.cl (accessed 11.6.18).

Flores Grandez, V., 2010. Modelo conceptual hidrogeológico de la cuenca del Salar del Huasco. Pontificia Universidad Catolica de Chile.